Theoretical Analysis of Regional Groundwater Flow: 1. Analytical and Numerical Solutions to the Mathematical Model

R. ALLAN FREEZE

Water Research Branch, Department of Mines and Technical Surveys Calgary, Alberta, Canada

P. A. WITHERSPOON

Department of Civil Engineering, University of California, Berkeley

Abstract. It is possible to represent steady-state regional groundwater flow in a three-dimensional, nonhomogeneous, anisotropic basin by a mathematical model. The numerical finite-difference approach can be used to solve the general case; the analytical separation of variables technique is restricted to two-dimensional layered mediums. The numerical method is more versatile, mathematically simpler, and well suited to computer oriented methods of data storage. Computer results are in the form of plotted potential nets from which flow patterns can be constructed. (Key words: Groundwater; computers, digital; drainage basin characteristics)

NOMENCLATURE

Analytical solutions

$c_1, c_2, \cdots c_{k+1}$,	slopes of various straight line segments in generalized water-table configuration.
g,	acceleration due to gravity.
K,	permeability.
K_1,	permeability of layer 1.
K_2,	permeability of layer 2.
K_3,	permeability of layer 3.
p,	pressure at given point.
p_0,	atmospheric pressure.
s,	lateral extent of basin.
v_x,	velocity (flux) in x-direction.
v_y,	velocity (flux) in y-direction.
v_z,	velocity (flux) in z-direction.
x,	horizontal coordinate direction.
$x_1, x_2, \cdots x_k$,	horizontal distance from $x = 0$ axis (left-hand vertical impermeable boundary) to each break in slope in the generalized water-table configuration.
z,	vertical coordinate direction.
z_0,	depth of basin.
z_1,	vertical distance from $z = 0$ axis (basal impermeable boundary) to contact layer between layer 1 and layer 2.
z_2,	vertical distance from $z = 0$ axis to contact between layer 2 and layer 3.
Φ,	hydraulic potential.
φ,	hydraulic head.
$\varphi_1(x, z)$,	hydraulic head at any point (x, z) in layer 1.
$\varphi_2(x, z)$,	hydraulic head at any point (x, z) in layer 2.
$\varphi_3(x, z)$,	hydraulic head at any point (x, z) in layer 3.
ρ,	density of water.

Numerical solutions

h,	nodal spacing in x-direction and y-direction.
(I, J),	nodal coordinates of any point (x, z) in two-dimensional field.
(I, K, J),	nodal coordinates of any point (x, y, z) in three-dimensional field.
$K_H(I, J)$,	horizontal permeability between node (I, J) and node $(I + 1, J)$.
$K_V(I, J)$,	vertical permeability between node (I, J) and node $(I, J + 1)$.
$K(I, K, J)$,	permeability associated with node (I, K, J); applies along 3 positive axes from (I, K, J) to neighboring nodes.
l,	nodal spacing in z-direction.
α,	h^2/l^2.
$\varphi(I, J)$,	potential at node (I, J).
$\varphi(I, K, J)$,	potential at node (I, K, J).
ω,	relaxation factor.

INTRODUCTION

In 1940, M. King Hubbert published his classic paper 'The Theory of Ground-Water Motion.' In this paper the physical laws governing the *steady-state* flow of groundwater were presented for the first time in their exact mathematical framework. At the same time a parallel course, in which formal mathematics was used to describe and predict *transient* hydrological phenomena, was being followed by many other hydrologists and applied mathematicians. The fundamental difference between the two approaches, apart from the time factor, was one of scale. Whereas Hubbert concerned himself mainly with the large-scale regional effects of his theory, workers in the transient field used the individual well as their unit of study. The immediate applicability of the latter studies in the determination of local aquifer conditions resulted in a preoccupation with the well and well field throughout the period 1935–1960 and led to the mathematical solution of almost all the meaningful problems in well hydraulics.

In the 1960's attention has again been turned to the regional situation, with the groundwater basin as the unit of hydrological study. The analysis of regional groundwater flow within a basin can be carried out using field techniques, such as geochemical correlation, piezometric interpretation, and geobotanical mapping [*Meyboom*, 1963], or using modeling techniques. One of the most versatile modeling methods is the so-called mathematical model, whereby exact groundwater flow patterns are obtained mathematically as solutions to formal boundary value problems.

Tóth [1962, 1963*b*] introduced this method and obtained solutions representing flow patterns in a two-dimensional section through a homogeneous basin for two separate water-table configurations. The actual formulas and quantitative results that were developed by Tóth are restricted to the specific cases that he considered.

The primary motivation for this study is to extend this approach to more general cases. The objective is therefore to develop a suitable mathematical model such that theoretical flow patterns can be obtained in a general three-dimensional, nonhomogeneous, anisotropic groundwater basin with any water-table configuration.

This study compares analytical and numerical solutions to the mathematical model that has been developed. In subsequent reports, the results of numerical solutions to a wide variety of modeled situations will be presented. These results will show the qualitative and quantitative effects on the groundwater flow system of (1) the configuration of the water table and (2) the configuration and variation in permeability of the underlying geological strata.

ASSUMPTIONS OF STUDY

1. There exists a three-dimensional closed hydrologic unit known as a groundwater basin that contains the entire flow paths followed by all water recharging the basin. It is bounded on the bottom by a horizontal impermeable basement, on the top by the ground surface, and on all sides by imaginary vertical impermeable boundaries representing the major groundwater divides. The flow pattern within the basin may be simple, involving only one recharge area and one discharge area, or complex, involving many.

2. All formations above the horizontal impermeable basement are permeable, and a reasonable estimate of any permeability contrasts can be made.

3. The upper boundary of the saturated flow system is the water table, whose configuration is known. It will be considered as an imaginary surface beneath ground level at which the absolute pressure is atmospheric.

4. The position of the water table is steady; that is, it does not fluctuate with time. This condition corresponds to what is referred to in the soil science literature [*Kirkham*, 1958] as the 'steady rainfall' case, or it might better be termed the 'steady recharge' case.

In defense of the above assumptions, a few comments and amplifications are necessary. The first two assumptions imply that one need not employ the terminology of 'confined' and 'unconfined' aquifers. All formations within the basin have some permeability, no matter how small. The *conditions* inferred by a 'confined' aquifer automatically arise when a high permeability bed is overlain by one with a permeability that is many magnitudes lower.

The imaginary vertical boundaries need not exist under every topographic high; indeed, this is one of the questions to be investigated. It has been found in the field, however, that the extent of groundwater basins is controlled by *major* topographic features. The horizontal impermeable basement is a matter of convenience, but, where necessary, the case of a sloping basement can be handled by introducing a wedge-shaped formation of very low permeability at the base of the model.

Knowledge of the water-table configuration is very important. In many locations, it will be valid to assume that the water table follows the topographic configuration. We recognize that this is not always the case, and, in areas where this relationship is doubtful, the water-table configuration must be determined independently.

The assumption that the water table is the upper boundary of flow is again a matter of convenience. This approach has two distinct advantages: (1) it is convenient in establishing the upper boundary of the model, and (2) it is easily measured in the field.

In the rigorous approach, the entire saturated-unsaturated system should be considered as continuous [*Luthin and Day,* 1955] and the ground surface should be used as the upper boundary of flow. The numerical solution presented in this paper is applicable to such a system, but one must have the variation of permeability with soil moisture content in the two-phase region. Such data are not often available, and, since the thickness of this air-water region relative to the total thickness of a groundwater basin will normally be very small, we are assuming that the effects of this upper flow regime can be neglected.

The fourth assumption of a steady-state water table is basic to this study and also the most liable to criticism. It should be thought of as a case of dynamic equilibrium in which the recharge to the water table (and discharge from the water table) is just the necessary amount to maintain it in its equilibrium position at every point along its length and at all times. Clearly, the assumption is not rigorously correct, but it can be defended on the basis of the following:

1. For the regional scale of most investigations, the difference of a few feet between high water and low water positions of the water table will have little effect on flow patterns.

2. The relative configuration of the water table usually remains the same throughout the cycle of fluctuations; that is, the high points remain the highest and low points remain the lowest.

Tóth [1963*a*], in reply to the objections of *Davis* [1963], states: '. . . the theory gives the *long term average* of the potential distribution. The theory does not yield quantitatively transient configurations of the flow pattern. . . .' He recommends using 'the mean position of the water table, the average of that of many dry and wet seasons' as the upper boundary of flow.

If either 1. or 2. is not true, then a succession of steady-states should be considered to approach the variability of the true situation. It may be necessary to run several models of a single basin, each with a different water-table configuration, representing the fluctuating position of the water table with time. The numerical solution presented below is directly applicable to such situations.

BASIS OF MATHEMATICAL MODEL

The existence of a three-dimensional groundwater flow system implies the existence of a corresponding three-dimensional potential field. The field in this case is the groundwater basin. The potential is the hydraulic potential [*Hubbert,* 1940]

$$\Phi = gz + \int_{p_0}^{p} dp/\rho \qquad (1)$$

For liquids, this potential reduces to

$$\Phi = gz + (p - p_0)/\rho \qquad (2)$$

where

Φ = hydraulic potential at any point in the field;
g = acceleration due to gravity;
z = elevation of given point above a standard horizontal datum;
p = pressure at given point;
p_0 = atmospheric pressure;
ρ = density of water.

The quantity $\varphi = \Phi/g$ is known as the hydraulic head and is measured in feet of water above a standard datum. Since φ equals the hydraulic potential divided by the constant g, it, too, is a potential quantity and consequently obeys all the laws of potential theory. It is measured in simple units that have geometrical significance in regional groundwater flow. Hence, φ will be used as the potential function throughout this study.

We can write Darcy's law for flow in the x-direction of an x, y, z coordinate system in a nonhomogeneous medium as

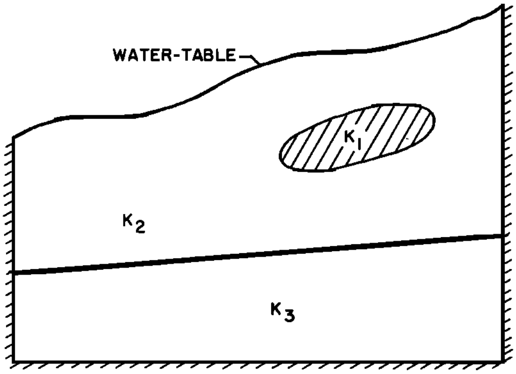

Fig. 1. A two-dimensional nonhomogeneous, isotropic physical model.

$$v_x = K(x, y, z)\ \partial\varphi/\partial x \tag{3}$$

where

v_x = velocity (flux) in x-direction;
$K(x, y, z)$ = permeability;
φ = hydraulic head.

Similar expressions can be written for flow in the other two coordinate directions. Equation 3 applies in isotropic mediums or in anisotropic mediums where the principal axes of the permeability tensor coincide with the coordinate axes.

For steady flow of an incompressible fluid, the equation of continuity takes the form

$$\partial v_x/\partial x + \partial v_y/\partial y + \partial v_z/\partial z = 0 \tag{4}$$

Substituting the appropriate form of Darcy's law (3) into (4) yields

$$\frac{\partial}{\partial x}\left[K(x, y, z)\frac{\partial\varphi}{\partial x}\right] + \frac{\partial}{\partial y}\left[K(x, y, z)\frac{\partial\varphi}{\partial y}\right] + \frac{\partial}{\partial z}\left[K(x, y, z)\frac{\partial\varphi}{\partial z}\right] = 0 \tag{5}$$

which is the steady-state form of Richards' equation [*Richards*, 1931]. For a saturated homogeneous medium, K is constant and (5) reduces to Laplace's equation

$$(\partial^2\varphi)/(\partial x^2) + (\partial^2\varphi)/(\partial y^2) + (\partial^2\varphi)/(\partial z^2) = 0 \tag{6}$$

A two-dimensional section through a nonhomogeneous but isotropic groundwater basin is shown in Figure 1. Establishing an x-z coordinate system in a similar but homogeneous basin would result in the mathematical model shown in Figure 2. Since there is no flow across the impermeable boundaries, we have $\partial\varphi/\partial x = 0$ along the vertical impermeable boundaries and $\partial\varphi/\partial z = 0$ along the horizontal base.

At any point on the water table, the pressure is atmospheric, so that the second term in (2) disappears. Therefore

$$\Phi = gz \tag{7}$$

or, in terms of the hydraulic head

$$\varphi = z \tag{8}$$

The hydraulic head (our potential function) at any point on the water table is thus equal to the elevation of the point above the standard datum (i.e., above the basal impermeable boundary denoted by $z = 0$). The values of z, and thus φ, along the water table are a function of x, so that

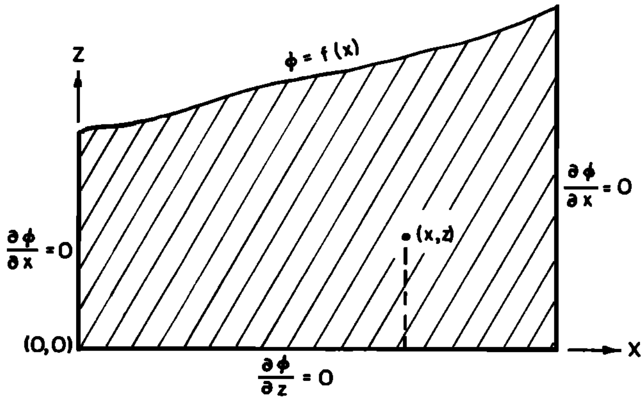

Fig. 2. A two-dimensional homogeneous, isotropic mathematical model.

the boundary condition along the water table can be represented by $\varphi = f(x)$, where $f(x)$ is the equation of the water-table configuration.

There are several methods of solving boundary value problems involving partial differential equations. These methods can be divided into two broad fields: analytical solutions involving the classic approach of formal mathematics; and the numerical solutions using the finite difference approach. Further development of the mathematical model will depend on the method of solution.

ANALYTICAL SOLUTIONS

In developing the formal analytical method of solution, three further restrictions to the mathematical model are necessary:

1. The method is restricted to two dimensions. The mathematical theory for the solution of boundary value problems in three dimensions is available, but in the case of regional groundwater flow it would necessitate representing the two-dimensional water-table surface by an algebraic expression $f(x, y)$. This representation would be impossible for any realistic water-table configuration. If, on the other hand, we consider a two-dimensional vertical section through the basin, the problem is reduced to finding an algebraic expression for the line representing the water table. In order that a two-dimensional section be considered representative of the basin, it must be taken perpendicular to the contours of the water table surface (i.e., parallel to the direction of slope of the water table).

2. Since analytical solutions to Richards' equation are unknown, we are restricted to the use of Laplace's equation. This restriction means that we cannot consider the general nonhomogeneous case of a permeability that varies continuously with the space variables. We can, however, treat layered cases where the basin consists of 2 or more horizontal geologic formations having different permeabilities. Each geological unit, however, must be homogeneous and isotropic with respect to permeability.

3. The available methods of solving Laplace's equation are limited to regions of regular shape. We cannot solve the problem in the region shown crosshatched in Figure 2, so that we must approximate the crosshatched region by a rectangle. This approximation is accomplished by applying the boundary condition $\varphi = f(x)$ along the upper surface of a rectangle instead of along the line representing the position of the water table. It should be noted that our problem is special in that the boundary condition $\varphi = f(x)$

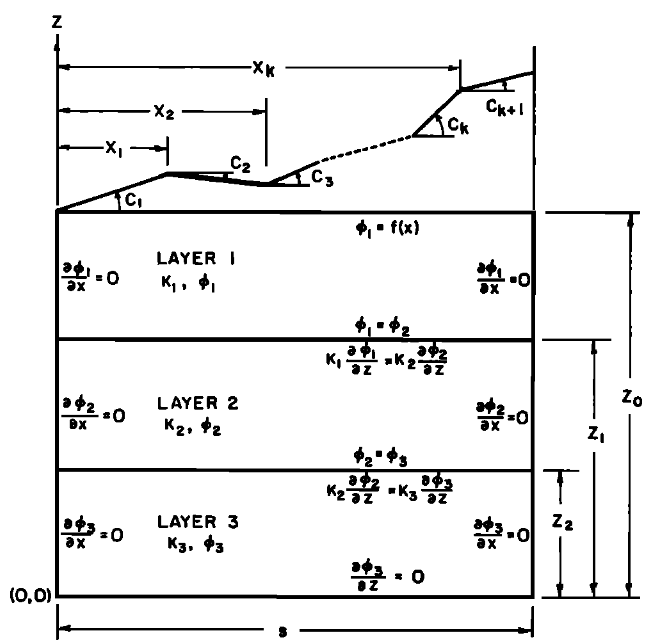

Fig. 3. Mathematical model for analytical method.

also defines the upper limit of the region in which we wish to solve the problem. By transferring the potential distribution $\varphi = f(x)$ onto the upper surface of the rectangle, we have in effect made the region of solution constant, but we may still represent any water-table configuration by varying $f(x)$. This representation ignores the small wedge of area that exists between the horizontal upper edge of the rectangle and the true position of the water table. The method is thus limited to regional slopes of a few degrees.

An analytical solution using the separation of variables technique and subject to the above restrictions will now be developed. The solution applies to a two-dimensional vertical section through a groundwater basin with three horizontal layers and a generalized water-table configuration. It is, of course, possible to develop a solution for n layers, but the three-layer case is the logical limit to which analytical solutions need be taken. The introduction of more boundary conditions would only result in an excessive amount of laborious mathematics and would lead to solutions so cumbersome that evaluation at enough points to define a flow pattern might prove prohibitive, even with the help of a digital computer. Numerical methods offer a far more suitable method of tackling these more complicated problems.

The boundary value problem to be solved is actually three interrelated problems (Figure 3). It is necessary to obtain three separate expressions for φ_1, φ_2, and φ_3, representing the hydraulic head in each of the three layers.

For layer 1, where the permeability is K_1, φ_1 must satisfy the Laplace equation

$$(\partial^2\varphi_1)/\partial x^2 + (\partial^2\varphi_1)/\partial z^2 = 0 \quad \text{where} \quad z_1 \leqq z \leqq z_0 \tag{9}$$

and the boundary conditions

$$\partial\varphi_1/\partial x(0, z) = 0 \tag{10}$$

$$\partial\varphi_1/\partial x(s, z) = 0 \tag{11}$$

$$K_1(\partial\varphi_1)/\partial z(x, z_1) = K_2\, \partial\varphi_2/\partial z(x, z_1) \tag{12}$$

$$\varphi_1(x, z_1) = \varphi_2(x, z_1) \tag{13}$$

$$\varphi_1(x, z_0) = f(x) \tag{14}$$

In layer 3, with permeability K_3, we have

$$(\partial^2\varphi_3)/\partial x^2 + (\partial^2\varphi_3)/\partial z^2 = 0 \quad \text{where} \quad 0 \leqq z \leqq z_2 \tag{15}$$

subject to

$$\partial\varphi_3/\partial x(0, z) = 0 \tag{16}$$

$$\partial\varphi_3/\partial x(s, z) = 0 \tag{17}$$

$$\partial\varphi_3/\partial z(x, 0) = 0 \tag{18}$$

$$K_2\, \partial\varphi_2/\partial z(x, z_2) = K_3\, \partial\varphi_3/\partial z(x, z_2) \tag{19}$$

$$\varphi_2(x, z_2) = \varphi_3(x, z_2) \tag{20}$$

In layer 2, with permeability K_2, φ_2 must satisfy

$$(\partial^2\varphi_2)/\partial x^2 + (\partial^2\varphi_2)/\partial z^2 = 0 \quad \text{where} \quad z_2 \leqq z \leqq z_1 \tag{21}$$

and the boundary conditions

$$\partial\varphi_2/\partial x(0, z) = 0 \tag{22}$$

$$\partial\varphi_2/\partial x(s, z) = 0 \tag{23}$$

as well as the four interlayer boundary conditions (12), (13), (19), and (20).

An expression for $f(x)$ in boundary condition 14, which represents a generalized water-table configuration, is

$$\begin{aligned} f(x) &= z_0 + c_1 x \qquad \text{for} \quad 0 \leqq x \leqq x_1 \\ &= z_0 + c_1 x_1 + c_2(x - x_1) \qquad \text{for} \quad x_1 \leqq x \leqq x_2 \\ &= z_0 + c_1 x_1 + c_2(x_2 - x_1) + c_3(x - x_2) \qquad \text{for} \quad x_2 \leqq x \leqq x_3 \\ &\;\vdots \\ &= z_0 + c_1 x_1 + c_2(x_2 - x_1) + \cdots + c_k(x_k - x_{k-1}) + c_{k+1}(x - x_k) \qquad \text{for} \quad x_k \leqq x \leqq s \end{aligned} \tag{24}$$

As shown in Figure 3, this expression represents a series of straight-line segments. The slopes $c_1, c_2, \cdots c_{k+1}$ and the positions of $x_1, x_2, \cdots x_k$ are arbitrary, so that any configuration of straight line segments can be represented.

By choosing an appropriate series of straight-line segments, one can represent any water-table configuration that is likely to be encountered in the field. We also approximated the curvilinear water tables such as *Tóth*'s [1963b] sine curve and obtained potential patterns that were identical with his.

Applying boundary conditions 10 and 11 to equation 9, boundary conditions 22 and 23 to equation 21, and boundary conditions 16, 17, and 18 to equation 15 yields

$$\left.\begin{aligned}\varphi_1(x, z) &= \cos\frac{m\pi x}{s}\left[D\cosh\frac{m\pi z}{s} + E\sinh\frac{m\pi z}{s}\right]\\ \varphi_2(x, z) &= \cos\frac{m\pi x}{s}\left[B\cosh\frac{m\pi z}{s} + C\sinh\frac{m\pi z}{s}\right]\\ \varphi_3(x, z) &= A\cos\frac{m\pi x}{s}\cosh\frac{m\pi z}{s}\end{aligned}\right\}\quad m = 0, 1, 2, \cdots \tag{25}$$

where A, B, C, D, and E are arbitrary constants. By applying the interlayer boundary conditions 12, 13, 19, and 20 to 25 we obtain expressions for φ_1, φ_2, and φ_3 in terms of the single arbitrary constant A

$$\left.\begin{aligned}\varphi_1(x, z) &= A\cos\frac{m\pi x}{s}\left[\cosh\frac{m\pi z}{s}(U) + \sinh\frac{m\pi z}{s}(Y)\right]\\ \varphi_2(x, z) &= A\cos\frac{m\pi x}{s}\left[\cosh\frac{m\pi z}{s}(W) + \sinh\frac{m\pi z}{s}(V)\right]\\ \varphi_3(x, z) &= A\cos\frac{m\pi x}{s}\cosh\frac{m\pi z}{s}\end{aligned}\right\}\quad m = 0, 1, 2, \cdots \tag{26}$$

where W, V, U, and Y are functions of m, z_1, z_2, K_1, K_2, K_3, and s and are defined below. Each potential expression represents an infinite number of solutions corresponding to the values of $m = 0, 1, 2, \cdots$ Since Laplace's equation is linear, we may sum these solutions and apply Fourier series theory. We can determine an expression for the arbitrary constant A_m by applying the final boundary condition 14, with $f(x)$ represented by the generalized water-table configuration 24. The final solution is

$$\left.\begin{aligned}\varphi_1(x, z) &= \frac{A_0}{2} + \sum_{m=1}^{\infty} A_m\cos\frac{m\pi x}{s}\left[\cosh\frac{m\pi z}{s}(U) + \sinh\frac{m\pi z}{s}(Y)\right]\\ \varphi_2(x, z) &= \frac{A_0}{2} + \sum_{m=1}^{\infty} A_m\cos\frac{m\pi x}{s}\left[\cosh\frac{m\pi z}{s}(W) + \sinh\frac{m\pi z}{s}(V)\right]\\ \varphi_3(x, z) &= \frac{A_0}{2} + \sum_{m=1}^{\infty} A_m\cos\frac{m\pi x}{s}\cosh\frac{m\pi z}{s}\end{aligned}\right\}\quad m = 0, 1, 2, \cdots \tag{27}$$

where

$$A_0 = \frac{1}{s}\left[z_0 s + \frac{c_{k+1}}{2}s^2 + \sum_{l=1}^{k}(c_{l+1} - c_l)\left(\frac{x_l^2}{2} - x_l s\right)\right]$$

$$A_m = \frac{2}{sQ}\left[\left(\frac{s}{m\pi}\right)^2\left\{c_{k+1}\cos m\pi - c_1 + \sum_{l=1}^{k}(c_l - c_{l+1})\cos\frac{m\pi x_l}{s}\right\}\right]$$

$$W = \cosh^2(m\pi z_2/s) - K_3/K_2\sinh^2(m\pi z_2/s)$$

$$V = (1 - W)/(\tanh(m\pi z_2/s))$$

$$T = \cosh^2(m\pi z_1/s) - K_2/K_1\sinh^2(m\pi z_1/s)$$

$$R = (1 - T)/\tanh(m\pi z_1)/s$$

$$U = (W)(T) + \cosh\frac{m\pi z_1}{s}\sinh\frac{m\pi z_1}{s}(V)\left(1 - \frac{K_2}{K_1}\right)$$

$$Y = (W)(R) + (V)(1 + K_2/K_1 - T)$$

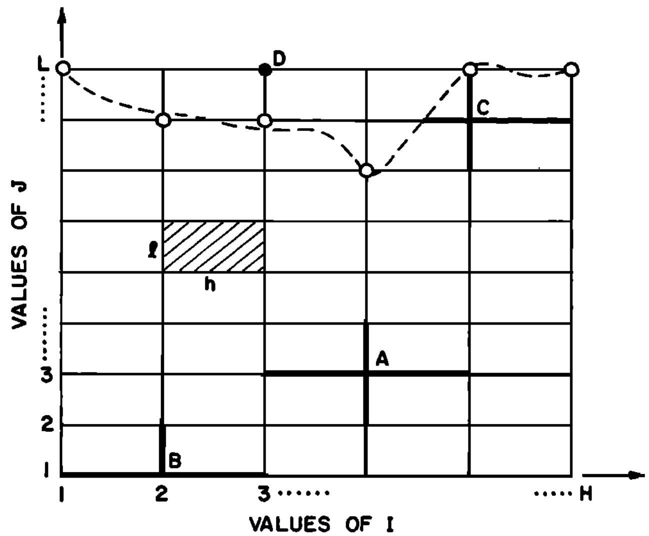

Fig. 4. Mathematical model for numerical method.

$$Q = \cosh (m\pi z_0/s)(U) + \sinh (m\pi z_0/s)(Y)$$

Each of the expressions 27 satisfies Laplace's equations and the appropriate boundary conditions. A detailed development of the mathematics is included in *Freeze* [1966].

It is, of course, possible to reduce the general solution to simpler cases. For example, letting $K_1 = K_2 = K_3$ in 27, we arrive at the solution for the homogeneous case, and the resulting expressions for φ_1, φ_2, and φ_3 are all identical to one another. If we let the water-table configuration be a uniform slope above a homogeneous basin, then $k = 0$ and $c_1 = c_{k+1} = c$ in (24). The result is identical to that obtained by *Tóth* [1962] for this case.

Equation 27 is the analytical solution to the two-dimensional three-layer problem with generalized water-table configuration and has been programmed in Fortran IV language for solution on a digital computer. The required input data are the values of the parameters that describe the geometry and properties of the model. The output is in the form of tables of values of the potential φ at a specified number of points in the field. In addition, a subroutine has been written, for use on an off-line plotter, that contours the resulting values of φ and produces a plotted equipotential net. Complete details can be found in *Freeze* [1966].

Figure 7A shows a solution obtained using the analytical method. The heavy dashed line represents the water-table configuration. The lighter dashed lines within the field are the plotted equipotential lines. The direction of groundwater flow is indicated qualitatively by the random flowlines shown. More of the details of this problem will be discussed below after the numerical solutions have been presented.

NUMERICAL SOLUTIONS

The three limitations placed on the mathematical model by the analytical solution are all removed in the numerical method. Therefore, it is possible to obtain potential patterns for a nonhomogeneous, anisotropic basin modeled in two or three space variables. It should be noted that in the initial development (Equations 3, 4, and 5) and in the numerical derivation to follow, the principal axes of the permeability tensor in the anisotropic case are assumed to coincide with the coordinate axes. However, by using the concept of the permeability tensor ellipsoid [*Liakopoulos*, 1965], the numerical method can easily be adapted to cases where the principal directions of anisotropy are different from the coordinate directions. Consider first the two-dimensional case.

In any numerical technique for solving a partial differential equation, the continuum of points (x, z) making up the field and its boundaries is replaced by a finite set of points (x_p, z_p) arranged in a grid over the region. The partial differential equation 5 that determines

$\varphi(x, z)$ over the field is then replaced by a finite system of simultaneous linear equations, one equation for each meshpoint. This process is known as discretization, and the resulting equations are finite-difference equations. If a mesh containing n nodes is used, the value of φ at each of these n points is determined by the solution of the system of n simultaneous linear finite-difference equations. The resulting value $\varphi(x_p, z_p)$ for the meshpoint (x_p, z_p) is considered as a representative value of $\varphi(x, z)$ for a small two-dimensional region of nearby points (x, z) of the field.

A regular rectangular mesh (Figure 4) is well suited to the long shallow groundwater basins we wish to model. The mesh spacing is h in the x-direction, and l in the z-direction. The nodes are numbered: $I = 1, I = 2, \cdots I = H$ in the x-direction; $J = 1, J = 2, \cdots J = L$ in the z-direction. A node is designated by its coordinates (I, J).

Richards' equation 5 belongs to a class of equations known as quasi-plane-harmonic [*Southwell,* 1946]. Discretization of boundary value problems involving quasi-plane-harmonic partial differential equations can be carried out using the usual finite-difference approximations to the first- and second-order partial derivatives occurring in the equation. To develop the expression for the potential $\varphi(I, J)$ at any interior node (I, J) such as A (Figure 4) we use the notation of the stencil shown in Figure 5 and the following finite-difference approximations

$$[\partial\varphi(I - \tfrac{1}{2}, J)]/\partial x = [\varphi(I, J) - \varphi(I - 1, J)]/h \qquad (28)$$

$$[\partial\varphi(I + \tfrac{1}{2}, J)]/\partial x = [\varphi(I + 1, J) - \varphi(I, J)]/h \qquad (29)$$

The first term of the two-dimensional Richards' equation at the point A is then approximated by

$$\left\{\frac{\partial}{\partial x}\left[K(x, z)\frac{\partial\varphi}{\partial x}\right]\right\}_A = \frac{\left[K\dfrac{\partial\varphi(I - \frac{1}{2}, J)}{\partial x}\right] - \left[K\dfrac{\partial\varphi(I + \frac{1}{2}, J)}{\partial x}\right]}{h} \qquad (30)$$

Applying 28 and 29 to 30 and noting that by the notation of Figure 5 the permeability at $(I - ½, J)$ is $K_H(I - 1, J)$ and the permeability at $(I + ½, J)$ is $K_H(I, J)$, we are led to

$$\left\{\frac{\partial}{\partial x}\left[K(x, z)\frac{\partial\varphi}{\partial x}\right]\right\}_A = \left\{\frac{K_H(I - 1, J)[\varphi(I, J) - \varphi(I - 1, J)]}{h^2} - \frac{K_H(I, J)[\varphi(I + 1, J) - \varphi(I, J)]}{h^2}\right\} \qquad (31)$$

Similarly, the second term becomes

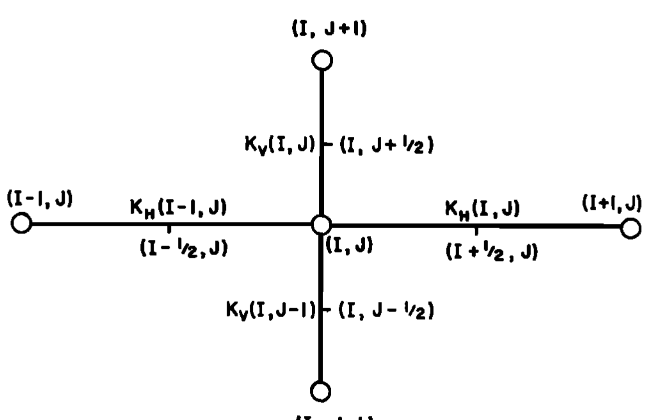

Fig. 5. Stencil for interior node used in development of finite-difference equation for two-dimensional, nonhomogeneous, anisotropic case.

$$\left\{\frac{\partial}{\partial z}\left[K(x, z)\frac{\partial \varphi}{\partial z}\right]\right\}_A = \frac{K_V(I, J-1)[\varphi(I, J) - \varphi(I, J-1)]}{l^2} - \frac{K_V(I, J)[\varphi(I, J+1) - \varphi(I, J)]}{l^2} \quad (32)$$

Substituting 31 and 32 into the two-dimensional form of Richards' equation and solving for φ (I, J) gives the finite-difference approximation of φ at the node (I, J)

$$\varphi(I, J) = \frac{\{K_H(I-1, J)\varphi(I-1, J) + K_H(I, J)\varphi(I+1, J) + \alpha K_V(I, J-1)\varphi(I, J-1) + \alpha K_V(I, J)\varphi(I, J+1)\}}{K_H(I-1, J) + K_H(I, J) + \alpha K_V(I, J-1) + \alpha K_V(I, J)} \quad (33)$$

where $\alpha = h^2/l^2$

For the homogeneous case with a square mesh, 33 reduces to the standard 5-point formula. In this case, $h = l$, $\alpha = 1$, and letting $K_H(I-1, J) = K_H(I, J) = K_V(I, J-1) = K_V(I, J)$ we have

$$\varphi(I, J) = \tfrac{1}{4}[\varphi(I-1, J) + \varphi(I+1, J) + \varphi(I, J-1) + \varphi(I, J+1)] \quad (34)$$

The finite-difference expressions for nodes on an external boundary must satisfy both Richards' equation and the boundary conditions at that point. To satisfy the boundary condition of no flow across the impermeable boundary at B (Figure 4), we imagine an image node a distance l below B, such that the value of φ at the image node equals the value of φ at the upper node in the stencil. The finite difference equation becomes

$$\varphi(I, J) = \frac{\{K_H(I-1, J)\varphi(I-1, J) + K_H(I, J)\varphi(I+1, J) + 2\alpha K_V(I, J)\varphi(I, J+1)\}}{\{K_H(I-1, J) + K_H(I, J) + 2\alpha K_V(I, J)\}} \quad (35)$$

Similar expressions can be developed for points on the vertical impermeable boundaries and at the corners.

The fourth boundary of the region is the water table. Its configuration is approximated by a series of straight-line segments joining the nodes nearest to the actual position of the water surface (Figure 4). The known values of φ (i.e., the elevation of the water table above the basal datum) are inserted into the system at these nodes. All nodes above the water table are given the value $\varphi = 0$ and are excluded from the iterative procedure used to solve the array of finite difference equations. All nodes below the water table are given an initial estimated value with which to begin the iterative procedure.

The possible presence of a steep water table as shown at C in Figure 4 necessitates the development of another finite difference expression. The standard 5-point formula (34) is not applicable since the point $(I-1, J)$ lies above the water table and φ $(I-1, J)$ has been arbitrarily set equal to zero. For this situation the Mikeladze formula for the improvement of boundary values is used [*Panov*, 1963]. The resulting expression for a square mesh and a homogeneous medium is

$$\varphi(I, J) = \tfrac{1}{18}[8\varphi(I-\tfrac{1}{2}, J) + 4\varphi(I+1, J) + 3\{\varphi(I, J+1) + \varphi(I, J-1)\}] \quad (36)$$

where by symmetry

$$\varphi(I-\tfrac{1}{2}, J) = \tfrac{1}{2}[\varphi(I, J+1) + \varphi(I-1, J-1)] \quad (37)$$

One can develop similar finite-difference expressions for three-dimensional studies. The mathematical model for the three-dimensional case is a nodal array with a mesh spacing of h in the x and y directions and a mesh spacing of l in the z direction. In plan (i.e., looking down from above at any x-y plane) the model may approximate any arbitrary areal extent of a groundwater basin. As in the two-dimensional case, the model is bounded on all sides by vertical impermeable boundaries and at the base by a horizontal impermeable boundary. The values of the potential (expressed as the head of water above the basal datum) along the water table are inserted in the appropriate nodes to approximate the position of the water-table surface. The stencil shown in Figure 6 is for an

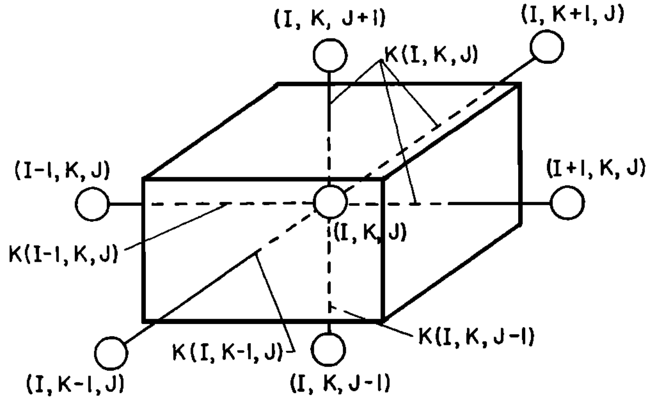

Fig. 6. Stencil for interior node in three-dimensional mesh for nonhomogeneous, isotropic medium.

interior node in a nonhomogeneous but isotropic medium. The permeability $K(I, K, J)$ associated with any node (I, K, J) is assumed to apply along the three positive axes extending from (I, K, J) to its neighboring nodes. The finite difference equation is

$$\varphi(I, K, J) = \frac{\begin{aligned}\{K(I, K, J)[\varphi(I+1, K, J) + \varphi(I, K+1, J) + \alpha\varphi(I, K, J+1)]\\ +K(I-1, K, J)\varphi(I-1, K, J)\\ +K(I, K-1, J)\varphi(I, K-1, J)+\alpha K(I, K, J-1)\varphi(I, K, J-1)\}\end{aligned}}{\{[2+\alpha]K(I, K, J) + K(I-1, K, J) + K(I, K-1, J) + \alpha K(I, K, J-1)\}} \tag{38}$$

It is a simple step to adapt (38) to the anisotropic case, with six different permeability values surrounding (I, K, J).

The system of simultaneous, linear, finite-difference equations may be solved using an iterative technique and the digital computer. *Forsythe and Wasow* [1960] provide an excellent development and discussion of the available iterative methods of solution. *Fayers and Sheldon* [1962] have considered the various methods in terms of their applicability to the study of the hydrodynamics of geologic basins. They recommend using the extrapolated Liebmann method of successive overrelaxation. In this method [*McCracken and Dorn,* 1964] the value of φ (I, J) obtained from the finite-difference expression is overcorrected as follows:

$$\varphi(I, J)^{(n)}_{\text{corr.}} = \omega\varphi(I, J)^{(n)} + (1 - \omega)\varphi(I, J)^{(n-1)}_{\text{corr.}} \tag{39}$$

where

$\varphi(I, J)^{(n)}_{\text{corr.}}$ = corrected value of $\varphi(I, J)$ for nth iteration;

$\varphi(I, J)^{(n)}$ = value of $\varphi(I, J)$ obtained from finite difference equation such as (33), (35), or (38) for nth iteration;

$\varphi(I, J)^{(n-1)}_{\text{corr.}}$ = corrected value of $\varphi(I, J)$ for previous iteration;

ω = relaxation factor, $1 < \omega < 2$.

Several authors [*Young,* 1954; *Forsythe and Wasow,* 1960; *Fayers and Sheldon,* 1962] have discussed the problem of choosing the optimum value of the relaxation factor ω. Unfortunately, there is no known method of arriving at the value for an elliptic partial differential equation with mixed boundary conditions and an irregular region. Trial and error, however, have shown that $\omega = 1.85$ gives a reasonable rate of convergence for the problem at hand.

When using a graded mesh involving several sizes of nodes, we were not always able to determine the optimum value of ω. In many such problems the iterative procedure diverged unless ω was set equal to 1.0 (the so-called Gauss-Seidel method). *Young* [1954] provides a detailed discussion of the properties necessary for convergence.

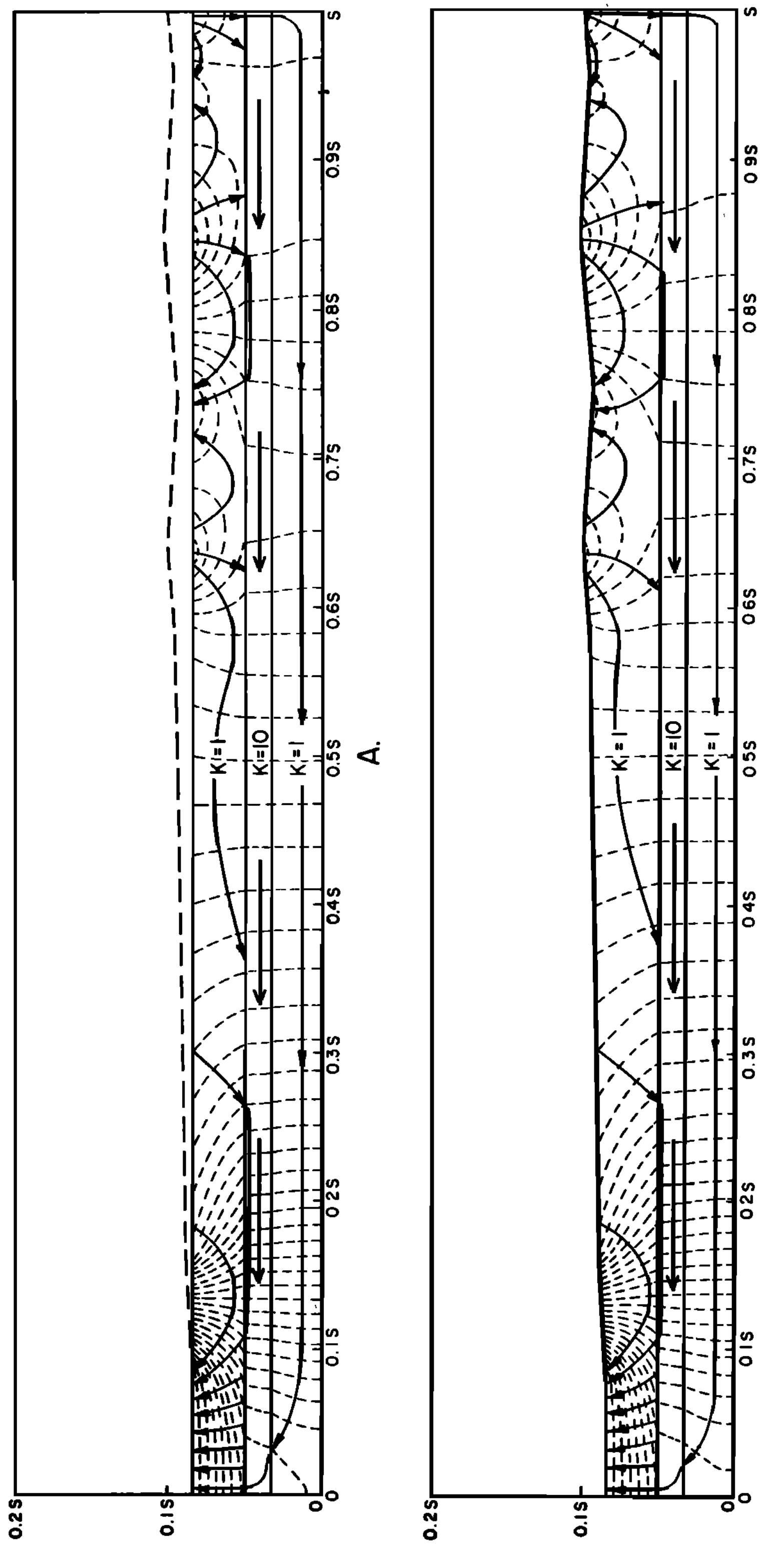

Fig. 7. Comparison of analytical solution (A) and numerical solution (B) to a hypothetical groundwater problem.

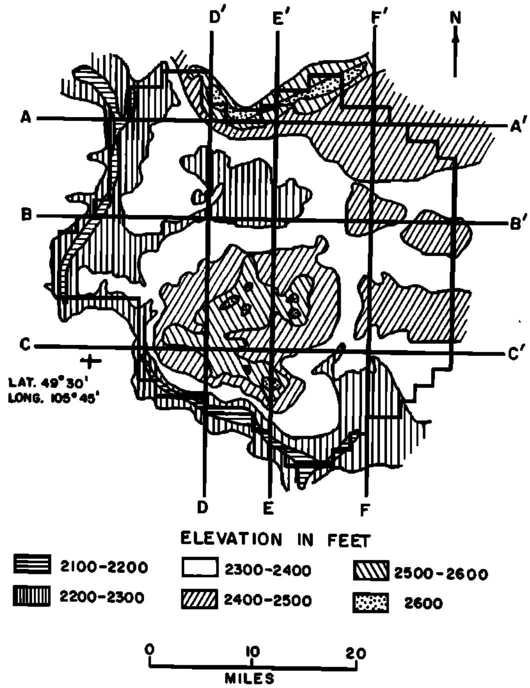

Fig. 8. Water-table topography for three-dimensional model of Old Wives Lake sub-basin near Assiniboia, Saskatchewan, Canada.

Figure 7B shows a solution for a regional groundwater problem obtained by the numerical method. The details of the computer programs used in obtaining this solution and many other numerical solutions are included in *Freeze* [1966].

COMPARISON OF ANALYTICAL AND NUMERICAL METHODS

The analytical and numerical methods described above are taken from two different branches of mathematics. In the analytical solution, the theory of partial differential equations and Fourier series is used; in the numerical method, recourse is made to the field of numerical analysis. The methods are therefore entirely independent. A high-speed digital computer is, of course, required in both methods, but the nature of the usage is different in each case.

An example of a matched analytical and numerical solution to the same two-dimensional problem is given in Figure 7. This is a hypothetical cross section across a nonhomogeneous groundwater basin involving three layers with a relatively more permeable layer in the middle. The assumed water-table configuration might result from a composite topography consisting of a major valley, a gentle constant slope, and hummocky terrain in the upstream portion of the basin.

The diagrams are true scale and dimensionless, i.e., all dimensions are given as fractions of '*s*,' the total length of the basin. The depth of the basin is about 8% of the length, and the average slope is just under 1°. The permeabilities shown for each layer are also dimensionless, because it is the permeability ratio that controls the potential field. The rectangular approximation was used in obtaining the analytical solution (Figure 7A) but not in the numerical solution (Figure 7B). The direction of groundwater flow is indicated by random flowlines. A complete flownet, having quantitative significance, could be constructed by drawing the flowlines orthogonal to the equipotential lines in such a way that they form curvilinear squares in the $K = 1$ layers and elongated rectangles (due to the law of refraction) in the $K = 10$ layer.

The results are qualitatively identical, although the closer approximation to the true basin inherent in the numerical method results in slight quantitative differences in the upstream half of the basin. Another reason for these minor deviations lies in the nature of the convergence inherent in each method. In the analytical solution, the result is in the form of an infinite series which, when programmed for the computer, must be represented by a finite number of terms. A small truncation error is thus introduced. In the numerical method, the iterative procedure converges to a solution. It, too, must be truncated when an acceptable tolerance has been reached. Therefore, a slight error due to incomplete convergence is always introduced.

An interpretation of the regional groundwater flow pattern shown in Figure 7 can be made in terms of the distribution of recharge and discharge areas along the surface of the water table (and therefore along the ground surface), the depth and lateral extent of the component subbasins in the region overlain by hummocky terrain, and the degree to which the zone of higher permeability acts as a major conductor of groundwater. The full hydrogeologic significance of this solution and other solutions will be the topic of future papers in this series.

An example of the application of the numerical method to a three-dimensional problem is shown in Figures 8 and 9. The area studied is a sub-basin of the Old Wives Lake internal drainage basin near Assiniboia, Saskatchewan,

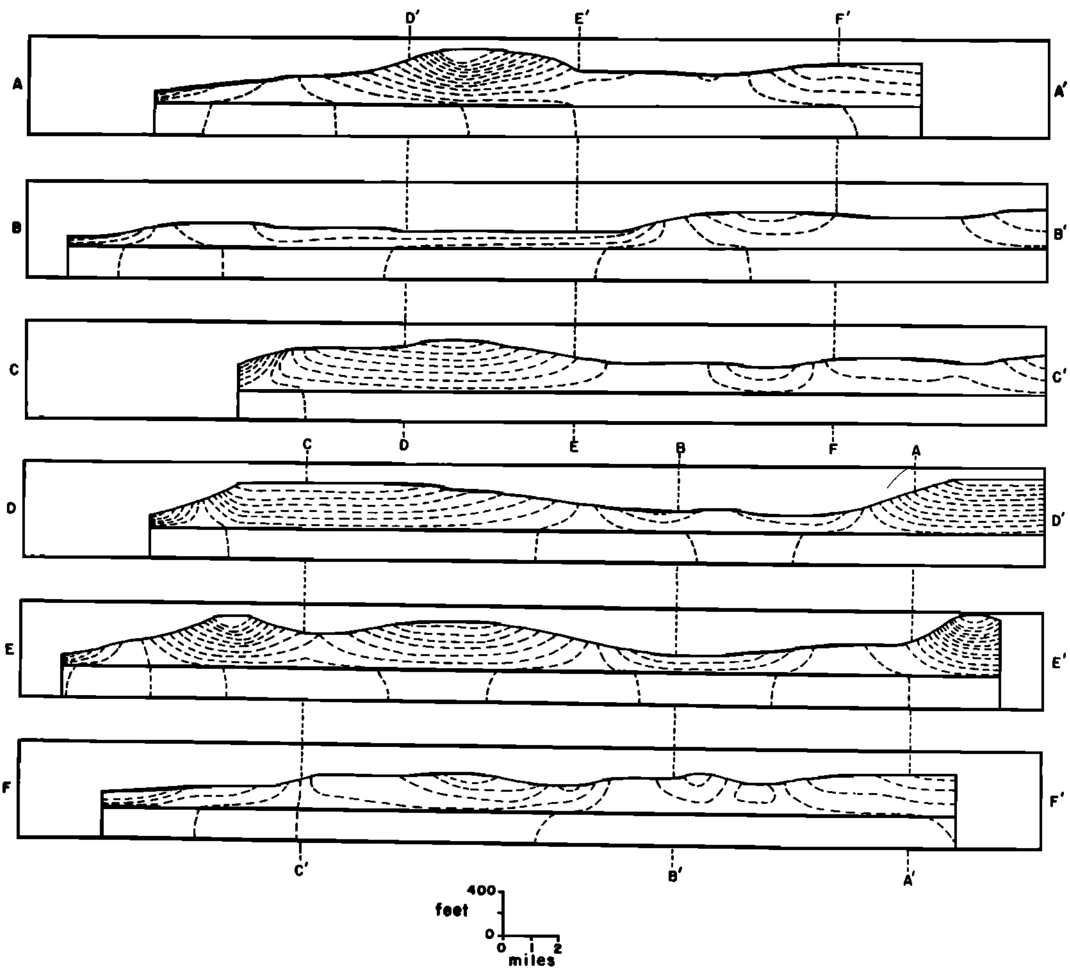

Fig. 9. Cross-sectional potential plots from three-dimensional model. Permeability of lower layer is 50 times that of upper layer. $K_H = 20\ K_V$ in both layers.

Canada. The water-table configuration for this area has been found from field observation to conform to the topography and is shown in Figure 8.

A nonhomogeneous, anisotropic model was required in addition to this complex water-table topography. The stratigraphy was simplified to two layers above an impermeable basement. A network of 6250 nodes was used ($25 \times 25 \times 10$). The permeability of the lower layer of constant thickness was taken to be 50 times that of the upper layer, which is of variable thickness. In the first analyses, each layer was assumed to be isotropic, but the results did not agree with field observation.

A solution that did give good agreement was finally obtained by using horizontal permeabilities 20 times the vertical in both layers. The results of the numerical solution for this anisotropic case are shown in the form of six vertical cross sections on Figure 9. Three of these cross sections (*AA′*, *BB′*, *CC′*) run in an east-west direction, and the other three (*DD′*, *EE′*, *FF′*) run north-south (see Figure 8). The points at which these cross sections intersect one another are also indicated on Figure 9. These results demonstrate the usefulness of numerical methods in elucidating the complex flow patterns that can arise in groundwater studies.

In general, flowlines and equipotential lines will not meet at right angles in anisotropic cases [*Liakopoulos*, 1965] or in cases where the results are represented on diagrams with an exaggerated vertical scale [*Van Everdingen*, 1963]. Caution must therefore be exercised in the delineation of flow patterns using potential nets obtained from the solution of mathematical models. In Figure 9, for example, the vertical exaggeration is 20 to 1. It would have to be reduced to 4.47 to 1 ($\sqrt{K_H/K_V} = 4.47$) before flowlines could be constructed orthogonal to the equipotential lines.

In theory, it is possible to represent any groundwater basin by a three-dimensional mathematical model. Figure 9 illustrates the type of solution that can be obtained. Our approach was limited by using computer programs that worked entirely within the core storage of an IBM 7094 having 32,000 cells. Using this machine, we were limited to 7500 nodes, which restricted the three-dimensional model to a network of $25 \times 25 \times 12$ nodes.

It is clear that this number of nodes is not sufficient to represent complicated water-table topographies or complex geological configurations for large basins. One approach to such situations is to select an appropriate series of vertical cross sections taken parallel to the direction of the dip of water table and to set up a series of two-dimensional models. Of course, if one has access to some of the newer computers with significantly larger core storage or to machines with auxiliary disk storage, then three-dimensional programs can be written that will overcome the above limitations.

CONCLUSIONS

It is our conclusion that the numerical method has several distinct advantages over the analytical method in solving mathematical models for groundwater basins:

1. The three restrictions of the analytical method are all removed: (a) the true shape of the field may be represented to a very close approximation. There is no limit on the regional water-table slope, because no rectangular approximation is required. (b) Richard's equation and Laplace's equation are handled in an identical fashion. The numerical method is thus capable of treating the general nonhomogeneous anisotropic case. (c) It is possible to construct three-dimensional models representing groundwater basins.

2. The numerical solution is general. Only one mathematical derivation is necessary to design a computer program that can handle any water-table configuration and any geologic configuration. The analytical method, on the other hand, requires a separate mathematical derivation for each change in the model. In addition, the mathematics involved in the numerical method is far simpler than that used in the analytical method.

3. For simple cases, the computer time is approximately the same for either method. As the complexity of the problem increases, however, the computer times involved in the analytical solutions increase, whereas those for the numerical programs remain more nearly constant.

4. *Remson et al.* [1965] have noted that

> a great advantage of the finite-difference digital computer approach is that it is compatible with machine oriented methods of data storage and retrieval.

They further state their belief that

> machine oriented storage will eventually be used for most types of groundwater data. It is likely that groundwater investigators will have libraries of programs capable of achieving certain types of solutions. It will be necessary only to take the data deck or tape for a given aquifer and the suitable program to a nearby computer to achieve a solution.

REFERENCES

Davis, S. N. Discussion of a paper by J. Tóth: A theory of groundwater motion in small drainage basins in central Alberta, Canada, *J. Geophys. Res., 68,* 2352–2353, 1963.

Fayers, F. J., and J. W. Sheldon, The use of a high-speed digital computer in the study of the hydrodynamics of geologic basins, *J. Geophys. Res., 67,* 2421–2431, 1962.

Forsythe, G. E., and W. R. Wasow, *Finite-Difference Methods for Partial Differential Equations,* John Wiley & Sons, 443 pp., 1960.

Freeze, R. A., Theoretical analysis of regional groundwater flow, Ph.D. thesis, University of California, Berkeley, 1966.

Hubbert, M. K., Theory of groundwater motion, *J. Geol., 48,* 785–944, 1940.

Kirkham, D., Seepage of steady rainfall through soils into drains, *Trans. Am. Geophys. Union, 39,* 892–908, 1958.

Liakopoulos, A. C., Variation of the permeability tensor ellipsoid in homogeneous anisotropic soils, *Water Resources Res.,* 1, 135–141, 1965.

Luthin, J. N., and P. R. Day, Lateral flow above a sloping water-table, *Soil Sci. Soc. Am. Proc., 19,* 406–410, 1955.

McCracken, D. D., and W. S. Dorn, *Numerical Methods and Fortran Programming,* John Wiley & Sons, 457 pp., 1964.

Meyboom, P., Patterns of groundwater flow in the prairie profile, *Natl. Res. Council Canada, Proc. Hydrol. Symp. 3: Groundwater,* 5–20, 1963.

Panov, D. J., *Formulas for the Numerical Solution of Partial Differential Equations by the Method of Differences,* Frederick Ungar Publishing Company, 133 pp., 1963.

Remson, I., C. A. Appel, and R. A. Webster, Ground-water models solved by a digital computer, *J. Hydraul. Div., Proc. Am. Soc. Civil Eng., 91,* HY 3, 133–147, 1965.

Richards, L. A., Capillary conduction of liquids through porous mediums, *Physics, 1,* 318–333, 1931.

Southwell, R. V., *Relaxation Methods in Theoretical Physics,* Oxford University Press, 248 pp., 1946.

Tóth, J., A theory of groundwater motion in small drainage basins in central Alberta, Canada, *J. Geophys. Res., 67,* 4375–4387, 1962.

Tóth, J., Reply to Davis (1963) re Tóth (1962), *J. Geophys. Res., 68,* 2354–2356, 1963*a*.

Tóth, J., A theoretical analysis of groundwater flow in small drainage basins, *J. Geophys. Res., 68,* 4795–4812, 1963*b*. (Also published in *Natl. Res. Council Canada, Proc. Hydrol. Symp. 3: Groundwater,* 75–96, 1963.)

Van Everdingen, R. O., Groundwater flow-diagrams in sections with exaggerated vertical scale, *Geol. Surv. Canada,* Paper 63-27, 1963.

Young, D., Iterative methods for solving partial differential equations of the elliptic type, *Trans. Am. Math. Soc.,* 76, 92–111, 1954.

(Manuscript received March 18, 1966.)